Intensity Distributions of Waves Transmitted through a Multiple Scattering Medium

Th. M. Nieuwenhuizen and M. C. W. van Rossum
Van der Waals-Zeeman Laboratorium, Universiteit van Amsterdam, Valckenierstraat 65, 1018 XE Amsterdam, The Netherlands
(Received 9 May 1994)

The distributions of the angular transmission coefficient and of the total transmission are calculated for multiple scattered waves. The calculation is based on a mapping to the known distribution of eigenvalues of the transmission matrix. The distributions depend on the profile of the incoming beam. The distribution function of the angular transmission has a stretched exponential decay. The total-transmission distribution grows log normally whereas it decays exponentially.

PACS numbers: 42.25.–p, 05.40.+j, 72.10.–d, 78.20.Dj

Transport through mesoscopic systems is a wide field of interest and is studied with a variety of waves: sound, microwaves, electrons, and light. The wave character leads to interference between the transmission channels causing large fluctuations. Therefore observables are not always characterized by mean values, but their entire distribution functions are of interest. This is particularly prominent in the distribution of eigenvalues of the transmission matrix. In the "metallic" regime where the dimensionless conductance g is large, the eigenvalues have a bimodal distribution peaked around 0 and 1 with a mean value $\ell/L \ll 1$, where ℓ is the mean free path and L is the thickness of the sample [1–3].

Three distinct optical transmission quantities can be measured. If a laser illuminates a diffuse medium, the transmitted signal consists of speckles. These speckles are the first quantity of interest. The intensities of the speckles obey in first approximation the Rayleigh law, which is a negative exponential distribution. In the mesoscopic regime interference modifies this distribution, as observed by Genack and Garcia at large intensities [4]. The leading correction was derived by Shnerb and Kaveh [5]. Also a crossover to a stretched exponential was observed [4], and an explanation was given by Kogan *et al.* [6].

The second quantity is the total transmission. It is obtained by integrating over the outgoing surface, thus collecting all speckles. When adding N independent channels, the law of large numbers predicts a Gaussian distribution with variance of the order $1/N$. However, interference broadens the variance to $L/\ell N$ [7]. This was confirmed in a recent experiment of de Boer *et al.* [8]. Also in computer simulations by Edrei, Kaveh, and Shapiro the Gaussian behavior was observed, with a crossover to a log-normal distribution for large disorder [9]. De Boer *et al.* also measured a small but clear deviation from a Gaussian, due to interference of three transmission channels.

The third quantity is the conductance, obtained by summing also over all incoming directions. For extensive discussion of its distribution, see Altshuler, Kravtsov, and Lerner [10].

The uncorrelated transport is in all cases given by diffusons, but the dominant processes correlating the channels are different for the three transmission quantities. This can already be seen by considering their autocorrelation functions [11,12]. Let T_{ab} be the angular transmission coefficient for a speckle spot b arising from an incoming wave a. Its correlator is called the C_1 correlation function. In accordance with the Rayleigh law, it is dominated by a *disconnected* diagram. The correlator $\langle T_a T_{a'} \rangle$ of the total transmission $T_a = \sum_b T_{ab}$ is called the C_2 correlation. It is dominated by the interference process mixing two incoming into two outgoing diffusons; it is a *connected, loopless* diagram. Because of the sum over the outgoing angles b, the amplitudes in the individual outgoing diffusons must have exactly the same phase. Loop diagrams contain a larger number of interference vertices than loopless ones and give corrections in $1/g$.

Finally, the correlator of the conductivity $T = \sum_{ab} T_{ab}$ is called C_3 correlation or universal conductance fluctuation. Because of the sum over both a and b also the amplitudes of the incoming diffusons must have pairwise the same phase. The diffusons interfere twice; it is a *connected loop* diagram [11]. Only in conductance measurements loop diagrams are leading.

We will generalize the results known for the autocorrelation functions, to arbitrary order. First the distribution function of the total transmission is calculated. Subsequently we apply these ideas to the statistics of the angular transmission coefficient. Consider a three dimensional slab with dimensions $W \times W \times L$ ($W \gg L$), with elastic scatterers at quenched random positions. Let us look at the transmission problem for a scalar plane wave with unit incoming flux in channel a,

$$\psi_a^{\rm in}(\mathbf{r}) = \frac{1}{\sqrt{Ak\mu_a}} \exp(i\mathbf{q}_a\rho + ik\mu_a z), \qquad z < 0, \quad (1)$$

where $A = W \times W$ denotes the area of the slab, k is the wave number, $\rho = (x, y)$ is the transversal coordinate, and $\mu_a = \sqrt{1 - \mathbf{q}_a^2/k^2} = \cos\theta_a$, with θ_a the angle with respect to the z axis. The precise form of the propagators was derived in Ref. [13]. An incoming diffuson has the

 0031-9007/95/74(14)/2674(4)$06.00 © 1995 The American Physical Society

form

$$\mathcal{L}_a^{\text{in}}(\mathbf{r}) = \frac{4\pi\tau_1(\mu_a)}{k\ell A\mu_a}\,\frac{L-z}{L}, \qquad (2)$$

where τ_1 describes the limit intensity of a semi-infinite system. We shall term the propagator summed over all incoming channels the *"total-flux diffuson"*:

$$\mathcal{L}^{\text{in}}(\mathbf{r}) \equiv \sum_a \mathcal{L}_a^{\text{in}}(\mathbf{r}) = \frac{4k}{\ell}\,\frac{L-z}{L}. \qquad (3)$$

In the bulk the difference between a total-flux diffuson and a diffuson arising from plane wave incidence is just described by an overall factor ϵ_a,

$$\mathcal{L}_a^{\text{in}}(\mathbf{r}) = \epsilon_a \mathcal{L}^{\text{in}}(\mathbf{r}), \qquad (4)$$

with $\epsilon_a \equiv \tau_1(\mu_a)\pi/k^2 A\mu_a$ satisfying the sum rule $\sum_a \epsilon_a = 1$. Similarly, the outgoing diffusons are

$$\mathcal{L}_b^{\text{out}}(\mathbf{r}) = \epsilon_b \mathcal{L}^{\text{out}}(\mathbf{r}), \qquad \mathcal{L}^{\text{out}}(\mathbf{r}) = \frac{k}{\ell}\,\frac{z}{L}. \qquad (5)$$

The wave is transmitted into outgoing channel b with transmission amplitude $t_{ab} = 2k\sqrt{\mu_a\mu_b}G_{ab}$ and transmission probability $T_{ab} \equiv |t_{ab}|^2$. The average total transmission is obtained by summation of all outgoing channels

$$\langle T_a\rangle = \left\langle \sum_b T_{ab} \right\rangle = \frac{\tau_1(\mu_a)\ell}{3L\mu_a}. \qquad (6)$$

The average conductance is given by

$$g \equiv \sum_a \langle T_a\rangle = \frac{k^2 A\ell}{3\pi L}, \qquad (7)$$

thus $\langle T_a\rangle = \epsilon_a g$, while one also has $\langle T_{ab}\rangle = \epsilon_a\epsilon_b g$ [13].

We consider the jth cumulant of T_a. In a diagrammatic approach this object has j transmission amplitudes t_{ab} and an equal number of Hermitian conjugates $t_{ba}^\dagger$. Let us fix the external diffusons in the term $t_{ab_1}t_{b_1a}^\dagger t_{ab_2}\cdots t_{ab_j}t_{b_ja}^\dagger$. Contributions to the sum over b_i only come from diagrams where the amplitudes of the outgoing diffusons have exactly the same phase. These are the diagrams where the lines with equal b_i are paired into diffusons. The outgoing diffusons are fixed now. For connected diagrams there are $(j-1)!$ distinct choices for pairing the incoming amplitudes. Next we factor out the incoming and outgoing diffusons and group the remainder of the diagrams into a skeleton K. Using Eq. (4) we obtain

$$\langle T_a^j\rangle_{\text{con}} = \epsilon_a^j (j-1)! \int d\mathbf{r}_1\, d\mathbf{r}_1' \cdots d\mathbf{r}_j\, d\mathbf{r}_j' \mathcal{L}^{\text{in}}(\mathbf{r}_1) \times \mathcal{L}^{\text{out}}(\mathbf{r}_1')\cdots\mathcal{L}^{\text{in}}(\mathbf{r}_j)\mathcal{L}^{\text{out}}(\mathbf{r}_j')K(\mathbf{r}_1,\mathbf{r}_1',\cdots,\mathbf{r}_j,\mathbf{r}_j'). \qquad (8)$$

The integral just describes

$$\langle \mathrm{Tr}(tt^\dagger)^j\rangle \equiv \sum_{a_1,b_1,\cdots,a_j,b_j} \langle t_{a_1b_1}t_{b_1a_2}^\dagger t_{a_2b_2}\cdots t_{a_jb_j}t_{b_ja_1}^\dagger\rangle. \qquad (9)$$

Indeed, for this quantity there is only one way to attach incoming and outgoing diffusons to K. The sums over the indices lead exactly to the total-flux diffusons in Eq. (8). We thus find

$$\langle T_a^j\rangle_{\text{con}} = (j-1)!\epsilon_a^j\langle \mathrm{Tr}(tt^\dagger)^j\rangle, \qquad (10)$$

which is the crucial step in the derivation. The eigenvalues T_n of the transmission matrix $t^\dagger t$ can be expressed as $T_n = 1/\cosh^2 L\gamma_n$. Under very general conditions [14] the distribution of the Lyapunov coefficients γ_n is uniform [1–3]. This implies that

$$\langle \mathrm{Tr}\,(tt^\dagger)^j\rangle = \left\langle \sum_{n=1}^N T_n^j \right\rangle = g\int_0^1 \frac{dT}{2T\sqrt{1-T}}\,T^j. \qquad (11)$$

Normalizing with respect to the average, we introduce $s_a = T_a/\langle T_a\rangle$. The generating function of the connected diagrams is easily calculated,

$$\Phi_{\text{con}}(x) \equiv \sum_{j=1}^\infty \frac{(-1)^{j+1}x^j}{j!}\,\langle s_a^j\rangle_{\text{con}} = g\ln^2\left(\sqrt{1+x/g} + \sqrt{x/g}\right). \qquad (12)$$

Since the cumulants are solely given by connected diagrams, the distribution of s_a follows as

$$p(s_a) = \int_{-i\infty}^{i\infty}\frac{dx}{2\pi i}\exp[xs_a - \Phi_{\text{con}}(x)]. \qquad (13)$$

For large g and $s_a \approx 1$ we expand Φ to order x^2, to recover the Gaussian behavior found by Kogan *et al.* [6],

$$p(s_a) \approx \sqrt{\frac{3g}{4\pi}}\exp\left[-\frac{3g}{4}(s_a-1)^2\right]. \qquad (14)$$

The integrand in Eq. (13) has a branch cut from $x = -g$ to $x = -\infty$. For $s_a \le 0$ the contour can be closed to the right and $p(s_a)$ vanishes. The shape for small s_a (and large g) is dominated by a saddle point. One finds essentially a log-normal growth:

$$p(s_a) \sim \exp\left[\frac{g}{4} - \frac{g}{4}\left(\ln\frac{2}{s_a} + \ln\ln\frac{2}{s_a} - 1\right)^2\right]. \qquad (15)$$

Also for large s_a we can apply steepest descent. Here one finds a simple exponential decay

$$p(s_a) \approx \exp\left(-gs_a + g\frac{\pi^2}{4}\right), \qquad s_a \gg 1. \qquad (16)$$

In Fig. 1 we present the distribution (13) for some values of g. At moderate g the deviation from a Gaussian is clearly seen.

So far we have considered the case of an incoming plane wave. In optical systems a Gaussian intensity profile is more realistic. For perpendicular incidence

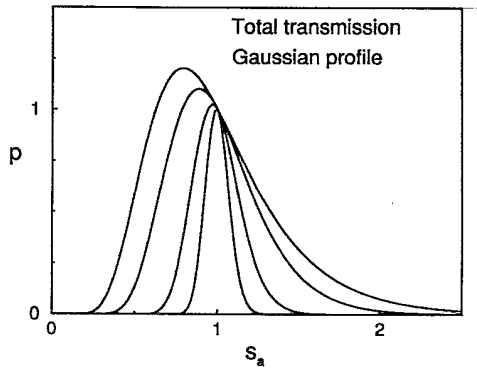

FIG. 1. Intensity distribution of the total transmission, in units of $\sqrt{3g/4\pi}$, versus the normalized intensity s_a for an incoming plane wave. $g = 2$, 4, 16, and 64 (upper to lower curves).

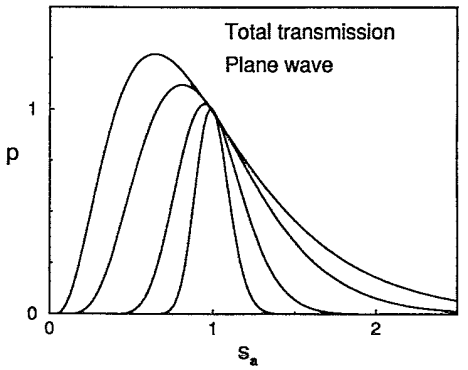

FIG. 2. Intensity distribution of the total transmission, in units of $\sqrt{3g/2\pi}$, versus the normalized intensity s_a for an incoming wave with Gaussian profile. $g = 2$, 4, 16, and 64 (upper to lower curves).

the incoming amplitude is $\psi^{\rm in}(\mathbf{r}) = W^{-1}\sum_a \phi(q_a)\psi_a^{\rm in}(\mathbf{r})$, where $\psi_a^{\rm in}(\mathbf{r})$ is the plane wave of Eq. (1), and where

$$\phi(q_a) = \sqrt{2\pi}\rho_0 \exp(-\tfrac{1}{4}\rho_0^2 q_a^2). \tag{17}$$

We consider the limit where the beam is much broader than the sample thickness ($\rho_0 \gg L$) but still much smaller than the transversal size of the slab ($\rho_0 \ll W$). (A smaller beam diameter complicates the problem; when incoming transverse momenta, which are of order $1/\rho_0$, become of the order $1/L$, the diffusons will take a momentum dependent form [8].) Because of integration over the center of gravity, each diagram involves a factor $A\delta_{\Sigma_q,\Sigma_{q'}}$. In the jth order term there occurs a factor

$$F_j = \frac{A}{A^{2j}} \sum_{q_1 q_1' \cdots q_j q_j'} \phi(q_1)\phi^*(q_1')\cdots\phi(q_j)\phi^*(q_j')\delta_{\Sigma_q,\Sigma_{q'}} = \int d^2\rho\ |\phi(\rho)|^{2j}. \tag{18}$$

For a plane wave we have $|\phi(\rho)| = \sqrt{A}$, and $F_j = A^{1-j}$. For the Gaussian profile we obtain

$$F_j = \frac{1}{j}\left(\frac{\pi\rho_0^2}{2}\right)^{1-j}. \tag{19}$$

It is thus convenient to identify $A_G = \frac{1}{2}\pi\rho_0^2$ with the effective area of a Gaussian beam. As compared to the plane wave case, the jth order term is smaller by a factor $1/j$ for a Gaussian profile. This implies for the generating function of the connected diagrams

$$\Phi_{\rm con}(x) = g\int_0^1 \frac{dy}{y} \ln^2\left(\sqrt{1+\frac{xy}{g}} + \sqrt{\frac{xy}{g}}\right). \tag{20}$$

For small s_a (and large g) there is again a log-normal saddle point. For large s_a the dominant shape of the decay is given by the singularity at $x = -g$ and again yields $p(s_a) \sim \exp(-gs_a)$. In Fig. 2 we present the distribution function for different values of g.

By expansion of $\Phi_{\rm con}$ we recover previous diagrammatic results for the second and third cumulants [8],

$$\langle s_a^2\rangle_{\rm cum} = \frac{2}{3g}, \qquad \langle s_a^3\rangle_{\rm cum} = \frac{12}{5}\langle s_a^2\rangle_{\rm cum}^2, \tag{21}$$

for a plane wave. For a Gaussian beam we recover

$$\langle s_a^2\rangle_{\rm cum} = \frac{1}{3g}, \qquad \langle s_a^3\rangle_{\rm cum} = \frac{16}{5}\langle s_a^2\rangle_{\rm cum}^2. \tag{22}$$

The latter relations were observed experimentally [8], confirming that the bimodal eigenvalue distribution, Eq. (11), is valid beyond quasi-1D [14]. As the results of Ref. [8] are based on loopless diagrams, the same should be true for Eq. (11) at any j. By including loop effects in Eq. (11) our theory can be extended. Indeed, Eq. (10) remains valid, as it comes from considering incoming and outgoing diffusons only.

We apply the same method for the distribution of the angular transmission coefficient. In the plane wave situation the average reads $\langle T_{ab}\rangle = \epsilon_a\epsilon_b g$. Let us count the number of connected loopless diagrams that contribute to $T_{ab}^j = t_{ab}t_{ba}^\dagger t_{ab}\cdots t_{ab}t_{ba}^\dagger$. In this case all pairings into outgoing diffusons contribute. This yields an extra combinatorical factor $j!$ in the jth moment,

$$\langle T_{ab}^j\rangle_{\rm con} = j!(j-1)!\epsilon_a^j\epsilon_b^j\langle {\rm Tr}(t^\dagger t)^j\rangle. \tag{23}$$

For the normalized angular transmission coefficient $s_{ab} = T_{ab}/\langle T_{ab}\rangle$, we introduce the following generating function of the connected diagrams:

$$\Psi_{\rm con}(x) \equiv \sum_{j=1}^{\infty} \frac{(-1)^{j-1}x^j}{j!\,j!}\langle s_{ab}^j\rangle_{\rm con}. \tag{24}$$

It is easy to see that $\Psi_{\rm con}(x) = \Phi_{\rm con}(x)$, with $\Phi_{\rm con}$ given by Eq. (12) for plane wave incidence and by Eq. (20) for a broad Gaussian beam, respectively. In contrast to the total-transmission distribution, the cumulants are not only given by the connected diagrams. Kogan *et al.* showed that the summation of the disconnected diagrams can

be done elegantly by performing an additional integral. Using this result one gets

$$p(s_{ab}) = \int_0^\infty \frac{dv}{v} \int_{-i\infty}^{i\infty} \frac{dx}{2\pi i} \exp\left(-\frac{s_{ab}}{v} + xv - \Psi_{\mathrm{con}}(x)\right). \tag{25}$$

The speckle intensity distribution is plotted in Fig. 3 for an incoming plane wave.

For large g and moderate s_{ab} we have $\Phi_{\mathrm{con}}(x) \approx x$ and we recover the Rayleigh law $p(s_{ab}) = \exp(-s_{ab})$. The leading correction is found by expanding in $1/g$,

$$p(s_{ab}) = e^{-s_{ab}}\left[1 + \frac{1}{3g}(s_{ab}^2 - 4s_{ab} + 2)\right]. \tag{26}$$

This was derived previously by Shnerb and Kaveh [5]; here we have related the prefactor of the correction term to the conductivity. Genack and Garcia fitted their data by this relation and found $g = 14.6$. Our Eq. (25) describes these data very well for $g = 14.4$.

For large s_{ab} we again apply steepest descent, and find

$$p(s_{ab}) \sim \exp(-2\sqrt{g s_{ab}}). \tag{27}$$

This stretched exponential tail differs from the form $p(s_{ab}) \sim \exp[-(81 g s_{ab}^2/16)^{1/3}]$ asserted by Kogan *et al.* Their findings are based on truncating $\Phi_{\mathrm{con}}(x)$ after order x^2, thus including only the simplest connected diagram. Taking the full generating function into account, we find a qualitatively different saddle point. Unfortunately, the intensities measured in Ref. [4] are not large enough to discriminate between our stretched exponential and the one of Kogan *et al.*

A Gaussian profile of the incoming beam leads to a different distribution with the same asymptotic behavior.

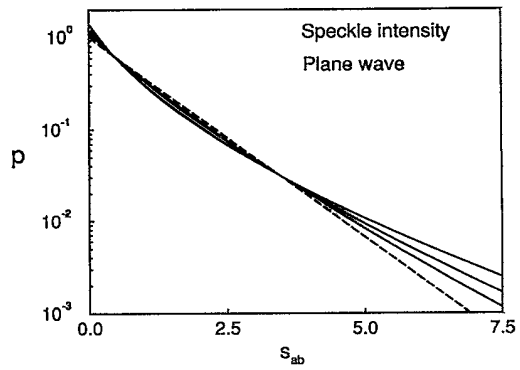

FIG. 3. Intensity distribution of speckles versus the normalized intensity s_{ab} for an incoming plane wave. $g = 2$, 4, and 8 (upper to lower curves at $s_{ab} = 5$). The dashed line corresponds to the Rayleigh law ($g = \infty$).

In conclusion, we have calculated the distribution function of the total amount of light transmitted through a disordered slab. It is related to the known distribution function of the eigenvalues of the transmission matrix. Next we have calculated the distribution of the angular transmission intensity. Here a deviation from Rayleigh statistics is found, of new stretched exponential form. Our calculations are in agreement with measurements of both total and angular resolved transmission.

As our results could be traced back on loopless diagrams, they constitute mean field expressions. Near the Anderson transition loop diagrams will change the distribution functions.

Discussions with I. V. Lerner, B. L. Altshuler, Yu. V. Nazarov, and J. F. de Boer are gratefully acknowledged. The research of Th. M. N. was supported by the Royal Netherlands Academy of Arts and Sciences (KNAW). This work was also sponsored by NATO (Grant No. CGR 921399).

[1] O. N. Dorokhov, Solid State Commun. **51**, 381 (1984).
[2] J. B. Pendry, A. MacKinnon, and A. B. Pretre, Physica (Amsterdam) **168A**, 400 (1990).
[3] A. D. Stone, P. A. Mello, K. A. Muttalib, and J.-L. Pichard, in *Mesoscopic Phenomena in Solids,* edited by B. L. Altshuler, P. A. Lee, and R. A. Webb (North-Holland, Amsterdam, 1991), Vol. 30, p. 369.
[4] N. Garcia and A. Z. Genack, Phys. Rev. Lett. **63**, 1678 (1989); A. Z. Genack and N. Garcia, Europhys. Lett. **21**, 753 (1993).
[5] N. Shnerb and M. Kaveh, Phys. Rev. B **43**, 1279 (1991).
[6] E. Kogan, M. Kaveh, R. Baumgartner, and R. Berkovits, Phys. Rev. B **48**, 9404 (1993).
[7] M. J. Stephen and G. Cwilich, Phys. Rev. Lett. **59**, 285 (1987).
[8] J. F. de Boer, M. C. W. van Rossum, M. P. van Albada, Th. M. Nieuwenhuizen, and A. Lagendijk, Phys. Rev. Lett. **73**, 2567 (1994).
[9] I. Edrei, M. Kaveh, and B. Shapiro, Phys. Rev. Lett. **62**, 2120 (1989).
[10] B. L. Altshuler, V. E. Kravtsov, and I. V. Lerner, in *Mesoscopic Phenomena in Solids* (Ref. [3]), p. 449.
[11] S. Feng, C. Kane, P. A. Lee, and A. D. Stone, Phys. Rev. Lett. **61**, 834 (1988).
[12] P. A. Mello, E. Akkermans, and B. Shapiro, Phys. Rev. Lett. **61**, 459 (1988).
[13] Th. M. Nieuwenhuizen and J. M. Luck, Phys. Rev. E **48**, 560 (1993).
[14] Yu. V. Nazarov, Phys. Rev. Lett. **73**, 134 (1994).